

## Elevated magma fluxes deliver high-Cu magmas to the upper crust

Cox, Daniel; Watt, Sebastian; Jenner, Frances E.; Hastie, Alan; Hammond, Samantha J.; Kunz, Barbara E.

DOI:  
[10.1130/G47562.1](https://doi.org/10.1130/G47562.1)

License:  
None: All rights reserved

*Document Version*  
Peer reviewed version

*Citation for published version (Harvard):*  
Cox, D, Watt, S, Jenner, FE, Hastie, A, Hammond, SJ & Kunz, BE 2020, 'Elevated magma fluxes deliver high-Cu magmas to the upper crust', *Geology*, vol. 48, no. 10, pp. 957-960. <https://doi.org/10.1130/G47562.1>

[Link to publication on Research at Birmingham portal](#)

### General rights

Unless a licence is specified above, all rights (including copyright and moral rights) in this document are retained by the authors and/or the copyright holders. The express permission of the copyright holder must be obtained for any use of this material other than for purposes permitted by law.

- Users may freely distribute the URL that is used to identify this publication.
- Users may download and/or print one copy of the publication from the University of Birmingham research portal for the purpose of private study or non-commercial research.
- User may use extracts from the document in line with the concept of 'fair dealing' under the Copyright, Designs and Patents Act 1988 (?)
- Users may not further distribute the material nor use it for the purposes of commercial gain.

Where a licence is displayed above, please note the terms and conditions of the licence govern your use of this document.

When citing, please reference the published version.

### Take down policy

While the University of Birmingham exercises care and attention in making items available there are rare occasions when an item has been uploaded in error or has been deemed to be commercially or otherwise sensitive.

If you believe that this is the case for this document, please contact [UBIRA@lists.bham.ac.uk](mailto:UBIRA@lists.bham.ac.uk) providing details and we will remove access to the work immediately and investigate.

'Elevated magma fluxes deliver high-Cu magmas to the upper crust'

1 **Title: Elevated magma fluxes deliver high-Cu magmas to the upper**  
2 **crust**

3  
4 **Authors:** Daniel Cox<sup>1\*</sup>, Sebastian F. L. Watt<sup>1</sup>, Frances E. Jenner<sup>2</sup>, Alan R. Hastie<sup>1</sup>,  
5 Samantha J. Hammond<sup>2</sup>, Barbara E. Kunz<sup>2</sup>

6  
7 **Affiliations:**

8 <sup>1</sup>School of Geography, Earth and Environmental Sciences, University of  
9 Birmingham, Birmingham, B15 2TT, U.K.

10 <sup>2</sup>School of Environment, Earth and Ecosystem Sciences, Open University, Walton  
11 Hall, Milton Keynes, MK7 6AA, U.K.

12

13 **\*Corresponding author:**

14 Daniel Cox: School of Geography, Earth and Environmental Sciences, University of  
15 Birmingham, Birmingham, B15 2TT, U.K. D.Cox@bham.ac.uk.

16

17 **ABSTRACT**

18 Porphyry Cu-Au ore deposits are globally associated with convergent  
19 margins. However, controls on the processing and distribution of the chalcophile  
20 elements (e.g., Cu) during convergent margin magmatism remain disputed. Here, we  
21 show that magmas feeding many Chilean stratovolcanoes fractionate high-Cu/Ag

‘Elevated magma fluxes deliver high-Cu magmas to the upper crust’

22 sulfides early in their crustal evolution. These magmas show evidence of lower-  
23 crustal garnet and amphibole crystallisation, and their degree of sulfide fractionation  
24 and Cu depletion increase with both crustal thickness and the extent of garnet  
25 fractionation. However, samples from a small proportion of volcanoes with elevated  
26 eruptive fluxes depart from this Cu-depleting trend, instead erupting Cu-rich  
27 magmas. This implies that at these atypical sites, elevated magma productivity and  
28 crustal throughput, potentially facilitated by ‘pathways’ exploiting major crustal fault  
29 systems, enables rapid magma transit, avoiding lower-crustal Cu-depleting sulfide  
30 fractionation and potentially playing an important role in porphyry ore genesis.

31

## 32 **INTRODUCTION**

33 Porphyry ore deposits are enriched in chalcophile metals (e.g., Cu, Ag) and  
34 are most frequently associated with areas above continental subduction zones  
35 (Sillitoe, 2010). The processes responsible for generating such deposits, formed in  
36 close association with upper-crustal arc-magmatic systems, are debated (Wilkinson,  
37 2013; Blundy et al., 2015; Lee and Tang, 2020). At oceanic island arcs, initial  
38 increases in magma Cu content are observed during crystallisation of hydrous  
39 magmas, until magnetite fractionation causes a decrease in magma  $fO_2$ , triggers  
40 sulfide fractionation and results in an abrupt decrease in magma Cu content (Jenner  
41 et al., 2010). Conversely, evolving continental arc magmas achieve sulfide saturation  
42 in the lower crust prior to magnetite crystallisation (Lee et al., 2012; Chiaradia, 2014;  
43 Georgatou et al., 2018; Cox et al., 2019). Earlier sulfide saturation during continental  
44 arc magmatism is attributed to either (1) pressure and temperature controls on  
45 sulfide stability (Jenner, 2017; Cox et al., 2019), and/or (2) garnet crystallisation (Cox

‘Elevated magma fluxes deliver high-Cu magmas to the upper crust’

46 et al., 2019; Lee and Tang, 2020). In Model 1, pressure and/or temperature effects  
47 enhance sulfide stability, permitting high- $fO_2$  magmas to fractionate sulfides near the  
48 base of the crust. In Model 2, lower-crustal garnet fractionation promotes sulfide  
49 saturation by depleting a magma in FeO, a consequence of the dependence of sulfur  
50 solubility on magma FeO content (O’Neill and Mavrogenes, 2002). However, the  
51 preferential uptake of  $Fe^{2+}$  relative to  $Fe^{3+}$  suggests that extensive lower-crustal  
52 garnet fractionation would eventually increase magma  $fO_2$  and therefore sulfur  
53 solubility (Lee and Tang, 2020). Lee and Tang (2020) suggest this garnet-driven  
54 auto-oxidation re-dissolves entrained sulfides, releasing Cu into the magma, which  
55 eventually partitions into magmatic fluids.

56 Both models suggest sulfides crystallise in the lower continental crust, forming  
57 Cu-rich cumulates, consistent with the Cu and Cu/Ag-depleted nature of the upper  
58 continental crust (Jenner, 2017; Chen et al., 2020). However, Model 2 provides a  
59 mechanism to transport ‘trapped’ Cu to upper crustal levels, a necessary step in  
60 porphyry ore formation (Lee and Tang, 2020). As garnet fractionation is restricted to  
61 magmas crystallising at high-pressures at the base of the continental crust (Alonso-  
62 Perez et al., 2009), Model 2 has been used to explain the dominance of porphyry Cu  
63 deposits at continental rather than oceanic arcs (Lee and Tang, 2020). An  
64 alternative, yet untested model involves magma ascent rapid enough to avoid  
65 substantial sulfide fractionation in the lower crust and therefore circumvent the need  
66 to identify a mechanism to rework and transport lower-crustal Cu-rich resources to  
67 upper-crustal levels (Jenner, 2017).

68 Here, we present major and trace element data [see Supplementary  
69 Materials] for volcanic rocks from several Pliocene-Holocene stratovolcanoes  
70 (Apagado, Hornopirén Villarrica, Quetrupillán, Lanín, San Pedro, Ollagüe) situated

## 'Elevated magma fluxes deliver high-Cu magmas to the upper crust'

71 along the Chilean segments of the Andean Volcanic Arc, South America (Fig. 1). We  
72 show that magmas ascending through thick ( $\geq 70$  km) crust fractionate a greater  
73 proportion of garnet and sulfide at the base of the continental crust than those  
74 transiting thinner ( $\leq 40$  km) crust. Thus, extensive garnet fractionation appears to  
75 enhance sulfide stability and Cu-depletion. We also identify instances where garnet  
76 and Cu-depleting sulfide fractionation appears minimal, specifically at locations of  
77 high magma flux.

## 78 **RESULTS AND DISCUSSION**

79 Copper concentrations and Cu/Ag of continental arc stratovolcanoes in  
80 Ecuador (Georgatou et al., 2018) and at Antuco Volcano, Chile (Cox et al., 2019)  
81 show positive trends with MgO, replicated here by our new Cu and Cu/Ag data for  
82 several Chilean stratovolcanoes (Fig. 2a, b). The decrease in Cu and Cu/Ag with  
83 decreasing MgO suggests removal of sulfides from many Chilean stratovolcano  
84 magmas across their entire compositional range (Cox et al., 2019). This is in contrast  
85 to oceanic arc-like magmas erupting through thinner crust (e.g., Manus Basin  
86 magmas, Fig. 2), which show sulfide saturation at later stages of differentiation ( $\sim 3$   
87 wt.% MgO), where sharp decreases in Cu and Cu/Ag coincide with the onset of  
88 magnetite fractionation (Jenner et al., 2010). Many of the primitive (high-MgO)  
89 Chilean stratovolcano samples have lower Cu/Ag relative to the global mid-ocean  
90 ridge basalt (MORB) array, suggesting that most magmas have been affected by  
91 some degree of sulfide removal in the lower continental crust, prior to ascent (Cox et  
92 al., 2019). This interpretation is consistent with the high-Cu/Ag nature of continental  
93 arc cumulates (Chen et al., 2020). Samples from Villarrica are an exception, having  
94 elevated Cu and Cu/Ag relative to other Chilean magmas and showing trends  
95 comparable to the low-pressure Manus Basin suite.

'Elevated magma fluxes deliver high-Cu magmas to the upper crust'

96 Unlike Manus Basin magmas, all our Chilean samples show evidence for  
97 garnet fractionation, having  $(Dy/Yb)_N$  ratios  $>1$  (Fig. 3a). 'Shape coefficients' [*cf.*  
98 O'Neill (2016)] are used to further evaluate the linear slope ( $\lambda_1$ ) and curvature ( $\lambda_2$ ) of  
99 normalised rare earth element patterns (Fig. 3b; see Supplementary Materials for  
100 discussion). The bulk of the Chilean stratovolcano dataset clusters tightly within a  
101 narrow range of  $\lambda_1$  (5 to 11) and at slightly higher values at a given  $\lambda_2$  than the  
102 MORB array and Manus Basin suite. These differences are consistent with garnet  
103 fractionation (Fig. 3a) from the Chilean magmas. Both Ollagüe and San Pedro  
104 stratovolcanoes erupt through extremely thick continental crust ( $\geq 70$  km) and display  
105 stronger garnet [*i.e.*, higher  $\lambda_1$  and  $(Dy/Yb)_N$ ; Fig. 3] and sulfide fractionation  
106 signatures than Chilean magmas erupting through thinner crust (*i.e.*,  $<40$  km). We  
107 suggest the strength of garnet and sulfide fractionation signatures at Ollagüe and  
108 San Pedro reflect differences in crustal thicknesses, which across their Pliocene-  
109 Holocene life cycle are unlikely to have differed significantly from those observed  
110 today (Mamani et al., 2010). Positive correlations between  $(Dy/Yb)_N$  and  $Dy/Dy^*$   
111 across our Chilean datasets suggest amphibole crystallisation followed garnet  
112 removal (Fig. 3a) at lower-crustal depths. Indeed, experimental studies have  
113 demonstrated that at  $\geq 1.2$  GPa ( $\geq 40$  km) garnet crystallises first at high temperatures  
114 ( $1000^\circ\text{C}$ ), followed by clinopyroxene and amphibole fractionation (Alonso-Perez et  
115 al., 2009).

116 Ollagüe and San Pedro, with the strongest garnet signatures, have the lowest  
117 Cu/Ag of the studied stratovolcanoes (Fig. 2). Thus, garnet fractionation appears to  
118 enhance crystalline sulfide fractionation and consequently, would result in the  
119 formation of more extensive sulfide cumulates at the base of thicker compared to  
120 thinner continental crust. Remobilisation of this Cu-rich reservoir could potentially

‘Elevated magma fluxes deliver high-Cu magmas to the upper crust’

121 account for the occurrence of some of the world’s largest porphyry Cu deposits in  
122 areas where the continental crust is thick and garnet fractionation is extensive.  
123 However, contrary to the model presented by Lee and Tang (2020), our data  
124 suggests that garnet fractionation does not appear to provide a sufficient enough  
125 increase in magma  $fO_2$  to re-dissolve sulfides. This is likely because the sulfide  
126 stability field extends beyond the  $fO_2$  range of magmas fractionating under lower-  
127 crustal pressure and temperature conditions (Matjuschkin et al., 2016; Nash et al.,  
128 2019). Thus, secondary mechanisms, such as injection of anomalously high  $fO_2$   
129 and/or sulfide undersaturated magmas, would be required to mobilise this deep Cu  
130 reservoir.

131 Similarities in Cu and Cu/Ag systematics between Villarrica and Manus Basin  
132 suites (Fig. 2) suggests that the Villarrica magmas achieved sulfide saturation  
133 following low-pressure magnetite fractionation and later in their evolutionary history  
134 (i.e., at lower MgO) than the other Chilean stratovolcano magmas. Samples from  
135 Villarrica show the least evidence of deep garnet fractionation among all our studied  
136 volcanoes, which contrasts with nearby samples erupting through similarly thick crust  
137 (Quetrupillán, Lanín). This implies fractionation of Villarrica magmas at mid- to  
138 upper-crustal pressures, where magnetite rather than garnet is stable (Matjuschkin  
139 et al., 2016). Thus, in contrast with the other Chilean stratovolcanoes, Villarrica  
140 magmas must have ascended rapidly enough to limit the effects of concomitant  
141 garnet and sulfide fractionation in the lower crust [i.e., before melt temperatures  
142 decreased to the 1000°C required for garnet fractionation (Alonso-Perez et al.,  
143 2009)].

144 Although uncommon, ‘Villarrica-type’ trends are not unique across Chile, with  
145 many samples from Llaima and the Puyehue–Cordon Caulle Volcanic Complex

## ‘Elevated magma fluxes deliver high-Cu magmas to the upper crust’

146 [PCCVC; Fig. 2a, S2] showing similar Cu enrichments (data from GeoROC  
147 database). At Villarrica, this appears to be a strongly localised effect; Quetrupillán  
148 and Lanín, part of the same across-arc volcanic chain, show no Cu-enrichment (Fig.  
149 2). Significantly, Villarrica and Llaima are the most active volcanic systems in the  
150 Southern Volcanic Zone (SVZ), based on historical records [64 and 50 eruptions  
151 since AD 1800, respectively (Global Volcanism Program, 2013)], while the PCCVC  
152 has also erupted several times in this period. Moreover, all three systems are  
153 characterised by an elevated eruptive flux, having volumes well in excess of 300  
154 km<sup>3</sup>, the largest among all volcanoes in the SVZ, and considerably greater than the  
155 average edifice volume (100 km<sup>3</sup>) (Volker et al., 2011). This suggests a link between  
156 high levels of magma productivity and conditions promoting rapid crustal ascent and  
157 the transport of high-Cu magmas to upper-crustal levels.

## 158 **PORPHYRY ORE FORMATION**

159 Higher degrees of mantle melting, consistent with geophysical evidence for  
160 elevated slab-fluid release beneath Villarrica and Llaima (Dzierma et al., 2012) and  
161 their high eruption rates, may facilitate their rapid magma ascent. A high magmatic  
162 flux may maintain elevated lower-crustal temperatures, preserving an open ‘pathway’  
163 through the lower crust and assisting rapid magma ascent, limiting the effects of  
164 magma stalling and storage on fractionation processes. Rapid magma ascent,  
165 limiting high temperature garnet fractionation (~1000°C) at the base of the  
166 continental crust, is potentially also facilitated by major fault systems [e.g., Liquiñe-  
167 Ofqui Fault Zone (LOFZ); Fig. 1], which are associated with many economic  
168 porphyry Cu deposits in northern Chile (Sillitoe, 2010). However, several Chilean  
169 volcanoes on the LOFZ show Cu depletions (e.g., Yate, Hornopirén, Lonquimay), so  
170 fault-related transport alone is insufficient to explain the ascent of Cu-rich magmas.



‘Elevated magma fluxes deliver high-Cu magmas to the upper crust’

171 Our new data identify an atypical scenario, contrasting with the usual  
172 chalcophile element cycle at continental arcs (i.e., formation of Cu-rich cumulates in  
173 the lower crust), that allows Cu-rich magmas to ascend to upper-crustal levels.  
174 Following ascent, processes inhibited in the lowermost continental crust may exploit  
175 the excess Cu in the system. For example, low-pressure S degassing causes sulfide  
176 undersaturation, destabilises sulfides and leads to melt Cu enrichment (Reekie et al.,  
177 2019). Hence, S-degassing during crystallisation of magmas with ‘Villarrica-style’  
178 low-pressure signatures might dissolve entrained sulfides, crystallised following  
179 magnetite fractionation [see also Wilkinson (2013) and Blundy et al. (2015) for  
180 additional mechanisms that could exploit low-pressure sulfide cumulates and aid ore  
181 formation]. Consequently, late-stage exsolved magmatic fluids might be enriched in  
182 Cu compared to those exsolved from typical continental arc magmas, which may  
183 enhance the ore-forming process.

184 As the pattern of elevated Cu concentrations is only observed at a small  
185 number of stratovolcanoes in the Chilean Andes, it could explain the sporadic and  
186 restricted distribution of porphyry ore deposits in the region. However, it is the thicker  
187 crust of the Central Andes that hosts many of the largest porphyry Cu deposits  
188 (Sillitoe, 2010), rather than the thinner crust of the Southern Andes. This could be  
189 because ore deposits, possibly forming beneath sites such as Villarrica today, are  
190 yet to be exposed. Additionally, the lack of ‘Villarrica-type’ Cu trends observed at  
191 currently-active stratovolcanoes in Central/Northern Chile may also partly reflect  
192 sampling bias in available datasets; most of our samples were collected from  
193 southern Chile and datasets including Cu analyses for central and northern Chile  
194 volcanoes are scant in the literature. Alternatively, the possibility remains that  
195 reworking of the more substantive Cu-rich cumulates at the base of the thickest crust

## 'Elevated magma fluxes deliver high-Cu magmas to the upper crust'

196 in Chile is still required to explain the dominance of porphyries in these regions (e.g.,  
197 through injection of anomalously sulfide undersaturated magmas, which would  
198 assimilate pre-existing sulfides). Regardless, we identify a mechanism to transport  
199 high-Cu magmas to the upper crust – rapid magma ascent rates. Together with the  
200 greater volume of magmas and therefore volume of Cu at sites of elevated magmatic  
201 fluxes, Villarrica-style magmatism might play a key role in enhancing ore formation.

202

### 203 REFERENCES

204 Alonso-Perez, R., Müntener, O., and Ulmer, P., 2009, Igneous garnet and amphibole  
205 fractionation in the roots of island arcs: Experimental constraints on andesitic  
206 liquids: *Contributions to Mineralogy and Petrology*, v. 157, p. 541–558.

207 Blundy, J., Mavrogenes, J., Tattitch, B., Sparks, S., and Gilmer, A., 2015, Generation  
208 of porphyry copper deposits by gas-brine reaction in volcanic arcs: *Nature*  
209 *Geoscience*, v. 8, p. 235–240.

210 Chen, K., Tang, M., Lee, C.A., Wang, Z., Zou, Z., Hu, Z., and Liu, Y., 2020, Sulfide-  
211 bearing cumulates in deep continental arcs: The missing copper reservoir: *Earth*  
212 *and Planetary Science Letters*, v. 531, p. 115971,  
213 doi:10.1016/j.epsl.2019.115971.

214 Chiaradia, M., 2014, Copper enrichment in arc magmas controlled by overriding  
215 plate thickness: *Nature Geoscience*, v. 7, p. 43–46.

216 Cox, D., Watt, S.F.L., Jenner, F.E., Hastie, A.R., and Hammond, S.J., 2019,  
217 Chalcophile element processing beneath a continental arc stratovolcano: *Earth*  
218 *and Planetary Science Letters*, v. 522, p. 1–11.

'Elevated magma fluxes deliver high-Cu magmas to the upper crust'

- 219 Davidson, J., Turner, S., and Plank, T., 2012, Dy/Dy\*: Variations arising from mantle  
220 sources and petrogenetic processes: *Journal of Petrology*, v. 54, p. 525–537.
- 221 Dzierma, Y., Rabbel, W., Thorwart, M., Koulakov, I., Wehrmann, H., Hoernle, K., and  
222 Comte, D., 2012, Seismic velocity structure of the slab and continental plate in  
223 the region of the 1960 Valdivia (Chile) slip maximum - Insights into fluid release  
224 and plate coupling: *Earth and Planetary Science Letters*, v. 331–332, p. 164–  
225 176.
- 226 Feigenson, M.D., Bolge, L.L., Carr, M.J., and Herzberg, C.T., 2003, REE inverse  
227 modelling of HSDP2 basalts: Evidence for multiple sources in the Hawaiian  
228 plume: *Geochemistry Geophysics Geosystems*, v. 4, p. 8706.
- 229 Georgatou, A., Chiaradia, M., Rezeau, H., and Wälle, M., 2018, Magmatic sulphides  
230 in Quaternary Ecuadorian arc magmas: *Lithos*, v. 296–299, p. 580–599.
- 231 Global Volcanism Program, 2013, *Volcanoes of the World*, v. 4.8.5. Venzke, E. (ed.):  
232 Smithsonian Institution, doi:<https://doi.org/10.5479/si.GVP.VOTW4-2013>.
- 233 Jenner, F.E., 2017, Cumulate causes for the low contents of sulfide-loving elements  
234 in the continental crust: *Nature Geoscience*, v. 10, p. 524–529.
- 235 Jenner, F.E., Arculus, R.J., Mavrogenes, J.A., Dyriw, N.J., Nebel, O., and Hauri,  
236 E.H., 2012, Chalcophile element systematics in volcanic glasses from the  
237 northwestern Lau Basin: *Geochemistry, Geophysics, Geosystems*, v. 13,  
238 doi:10.1029/2012GC004088.
- 239 Jenner, F.E., and O'Neill, H.S.C., 2012, Analysis of 60 elements in 616 ocean floor  
240 basaltic glasses: *Geochemistry, Geophysics, Geosystems*, v. 13, p. 1–11.
- 241 Jenner, F.E., O'Neill, H.S.C., Arculus, R.J., and Mavrogenes, J.A., 2010, The

'Elevated magma fluxes deliver high-Cu magmas to the upper crust'

- 242 magnetite crisis in the evolution of arc-related magmas and the initial  
243 concentration of Au, Ag and Cu: *Journal of Petrology*, v. 51, p. 2445–2464.
- 244 Lee, C.T.A., Luffi, P., Chin, E.J., Bouchet, R., Dasgupta, R., Morton, D.M., Le Roux,  
245 V., Yin, Q., and Jin, D., 2012, Copper systematics in arc magmas and  
246 implications for crust-mantle differentiation: *Science*, v. 336, p. 64–68.
- 247 Lee, C.T.A., and Tang, M., 2020, How to make porphyry copper deposits: *Earth and*  
248 *Planetary Science Letters*, v. 529, p. 115868.
- 249 Mamani, M., Wörner, G., and Sempere, T., 2010, Geochemical variations in igneous  
250 rocks of the Central Andean orocline (13°S to 18°S): Tracing crustal thickening  
251 and magma generation through time and space: *Bulletin of the Geological*  
252 *Society of America*, v. 122, p. 162–182.
- 253 Matjuschkin, V., Blundy, J.D., and Brooker, R.A., 2016, The effect of pressure on  
254 sulphur speciation in mid- to deep-crustal arc magmas and implications for the  
255 formation of porphyry copper deposits: *Contributions to Mineralogy and*  
256 *Petrology*, v. 171, p. 66, doi:10.1007/s00410-016-1274-4.
- 257 Nash, W.M., Smythe, D.J., and Wood, B.J., 2019, Compositional and temperature  
258 effects on sulfur speciation and solubility in silicate melts: *Earth and Planetary*  
259 *Science Letters*, v. 507, p. 187–198.
- 260 O'Neill, H.S.C., 2016, The smoothness and shapes of chondrite-normalized rare  
261 earth element patterns in basalts: *Journal of Petrology*, v. 57, p. 1463–1508.
- 262 O'Neill, H.S.C., and Mavrogenes, J.A., 2002, The Sulfide Capacity and the Sulfur  
263 Content at Sulfide Saturation of Silicate Melts at 1400°C and 1 bar: *Journal of*  
264 *Petrology*, v. 43, p. 1049–1087.

'Elevated magma fluxes deliver high-Cu magmas to the upper crust'

265 Reekie, C.D.J., Jenner, F.E., Smythe, D.J., Hauri, E.H., Bullock, E.S., and Williams,  
266 H.M., 2019, Sulfide resorption during crustal ascent and degassing of oceanic  
267 plateau basalts: *Nature Communications*, v. 10, p. 1–11.

268 Sillitoe, R.H., 2010, *Porphyry Copper Systems: Economic Geology*, v. 105, p. 3–41.

269 Stern, C.R., 2004, Active Andean volcanism: its geologic and tectonic setting:  
270 *Revista geológica de Chile*, v. 31, p. 161–206.

271 Tassara, A., and Echaurren, A., 2012, Anatomy of the Andean subduction zone:  
272 Three-dimensional density model upgraded and compared against global-scale  
273 models: *Geophysical Journal International*, v. 189, p. 161–168.

274 Volker, D., Kutterolf, S., and Wehrmann, H., 2011, Comparative mass balance of  
275 volcanic edifices at the southern volcanic zone of the Andes between 33 S and  
276 46 S: *Journal of Volcanology and Geothermal Research*, v. 205, p. 114–129.

277 Wessel, P., Luis, J.F., Uieda, L., Scharroo, R., Wobbe, F., Smith, W.H.F., and Tian,  
278 D., 2019, The Generic Mapping Tools version 6: *Geochemistry, Geophysics,*  
279 *Geosystems*, v. 20, p. 5556–5564.

280 Wilkinson, J.J., 2013, Triggers for the formation of porphyry ore deposits in  
281 magmatic arcs: *Nature Geoscience*, v. 6, p. 917–925.

282

283 **Figure captions:**

284 **Fig. 1.** Map showing the location of the Chilean stratovolcanoes investigated in the  
285 current study, Moho depth (red text) (Tassara and Echaurren, 2012), subducting slab  
286 age and Nazca Plate velocity (Stern, 2004). LOFZ: Liquiñe-Ofqui Fault Zone;

287 PCCVC: Puyehue – Cordon Caulle Volcanic Complex. Maps constructed using the  
288 Generic Mapping Tool (Wessel et al., 2019).

289

290 **Fig. 2.** Select bivariate plots of the Chilean stratovolcano datasets. Cu (a) and Cu/Ag  
291 (b) continually decrease with MgO (black arrows) in the continental arc stratovolcano  
292 datasets [including at Antuco; C19: data from Cox et al. (2019)]. This differs to the  
293 trend observed (blue arrows) in the Manus Basin sample suite [data from J12:  
294 Jenner et al. (2012)], where both Cu and Cu/Ag increase to a ~3 wt% MgO  
295 maximum before they plummet due to magnetite fractionation induced sulfide  
296 saturation [the onset of magnetite fractionation is identified by a sudden drop in the  
297 total Fe contents of the Manus Basin suite at ~4 wt.% MgO (panel c)]. Samples from  
298 Villarrica, and most analyses from Llaima and the Puyehue – Cordon Caulle  
299 Volcanic Complex (PCCVC) (data for all Chilean stratovolcanoes sourced from the  
300 GeoROC database, <http://georoc.mpch-mainz.gwdg.de/georoc>: accessed 25/01/20),  
301 have Cu contents elevated relative to other Chilean and Ecuadorian [data from G18:  
302 Georgatou et al. (2018)] stratovolcanoes and the global mid-ocean ridge basalt  
303 (MORB) array [J12] at a given MgO. Filtered Cu and MgO from the GeoROC  
304 Databases are collated in Supplementary Material S3. Ag analyses are unavailable  
305 from Llaima and PCCVC.

306

307 **Fig. 3.** Rare earth element (REE) systematics of the Chilean stratovolcano datasets.  
308 (a)  $(Dy/Yb)_N$  versus  $Dy/Dy^*$ , after Davidson et al. (2012) . All samples show evidence  
309 of an initial stage of garnet fractionation prior to more extensive amphibole  
310 fractionation, most strongly developed for volcanoes on thickest crust, and most

‘Elevated magma fluxes deliver high-Cu magmas to the upper crust’

311 weakly for Villarrica (the Manus Basin oceanic-crust samples show no evidence of  
312 garnet fractionation). Insets represent the expected REE patterns in each quadrant.  
313 (b) ‘Shape coefficients’, defined by O’Neill (2016);  $\lambda_1$ : linear slope of the REE  
314 pattern,  $\lambda_2$ : curvature of the REE pattern (outlined in Supplementary Materials). The  
315 red dashed tramlines highlight the field defined by mid-ocean ridge basalts (MORB)  
316 [data from Jenner and O’Neill (2012)]. Ocean island basalt (OIB; Hawaii) data are  
317 plotted to exemplify the offset related to garnet fractionation [data from Feigenson et  
318 al. (2003)]. The vectors ‘Amph fract.’ and ‘Grt fract.’ highlight expected fractionation  
319 trends for amphibole and garnet, respectively. 25 – 40 km and >70 km denote the  
320 thickness of the continental crust on which the stratovolcanoes are sat. C19: data for  
321 Antuco stratovolcano from Cox et al. (2019); J12: data for the Manus Basin (MB)  
322 magmas from Jenner et al. (2012).

323

324 **Acknowledgments:**

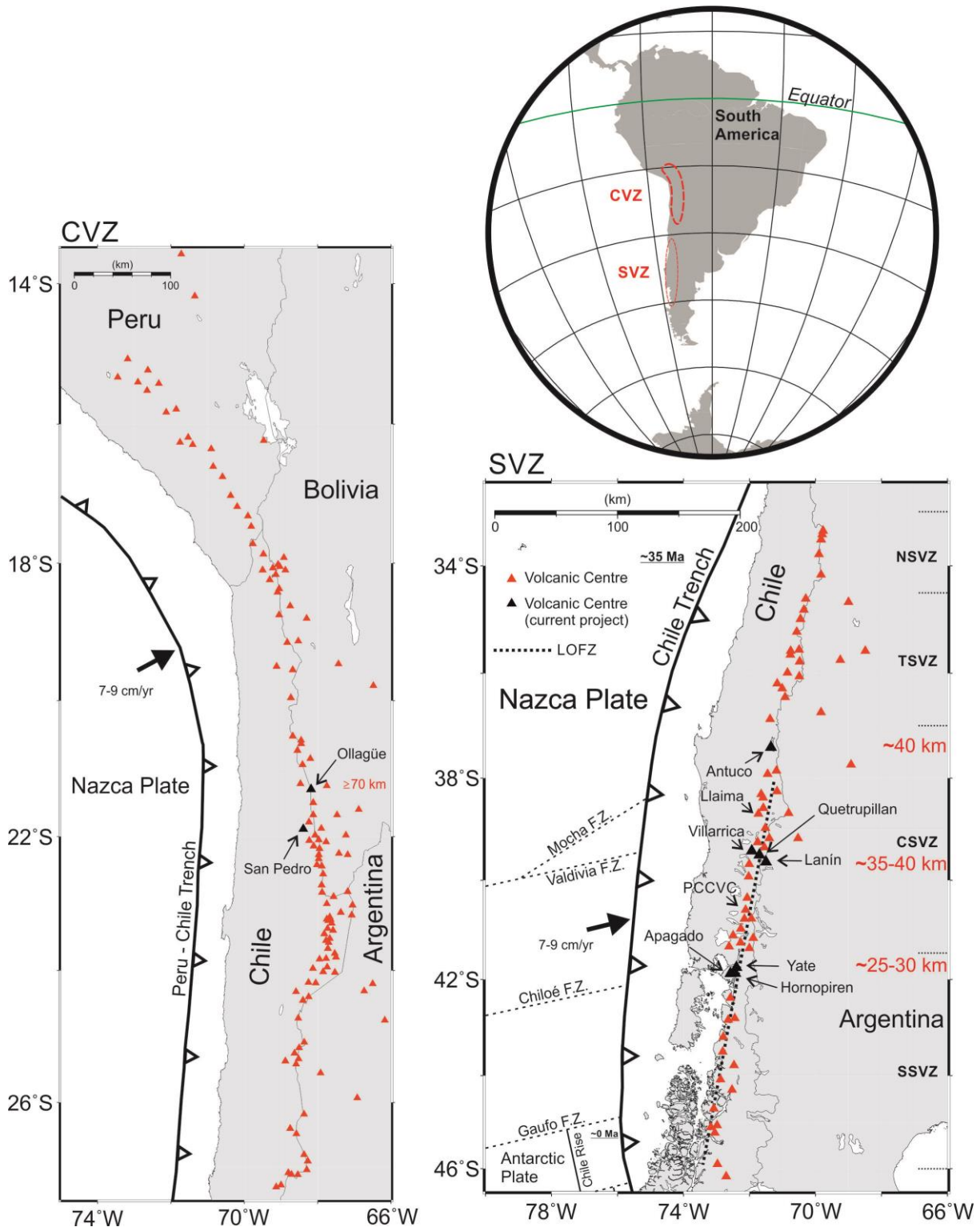
325 We thank Alvaro Amigo Ramos, Ginevra Chelli and David Cavell for fieldwork  
326 assistance and Iain McDonald (Cardiff University) and Lin Marvin-Dorland (University  
327 of Leicester) for laboratory support. We acknowledge funding for this work from the  
328 Natural Environment Research Council (NERC): NE/M000427/1 (Mantle volatiles:  
329 processes, reservoirs & fluxes), NE/M010848/1 [SoS Tellurium & Selenium Cycling  
330 & Supply ] and NE/P017045/1 [From Arc Magmas to Ore Systems]. All data are  
331 presented in the main manuscript or Supplementary Materials. Gerald Dickens  
332 (Editor) and three anonymous reviewers are thanked for their thorough and  
333 constructive comments during review, which greatly improved the manuscript.

334

'Elevated magma fluxes deliver high-Cu magmas to the upper crust'

335 Figure 1

336



337

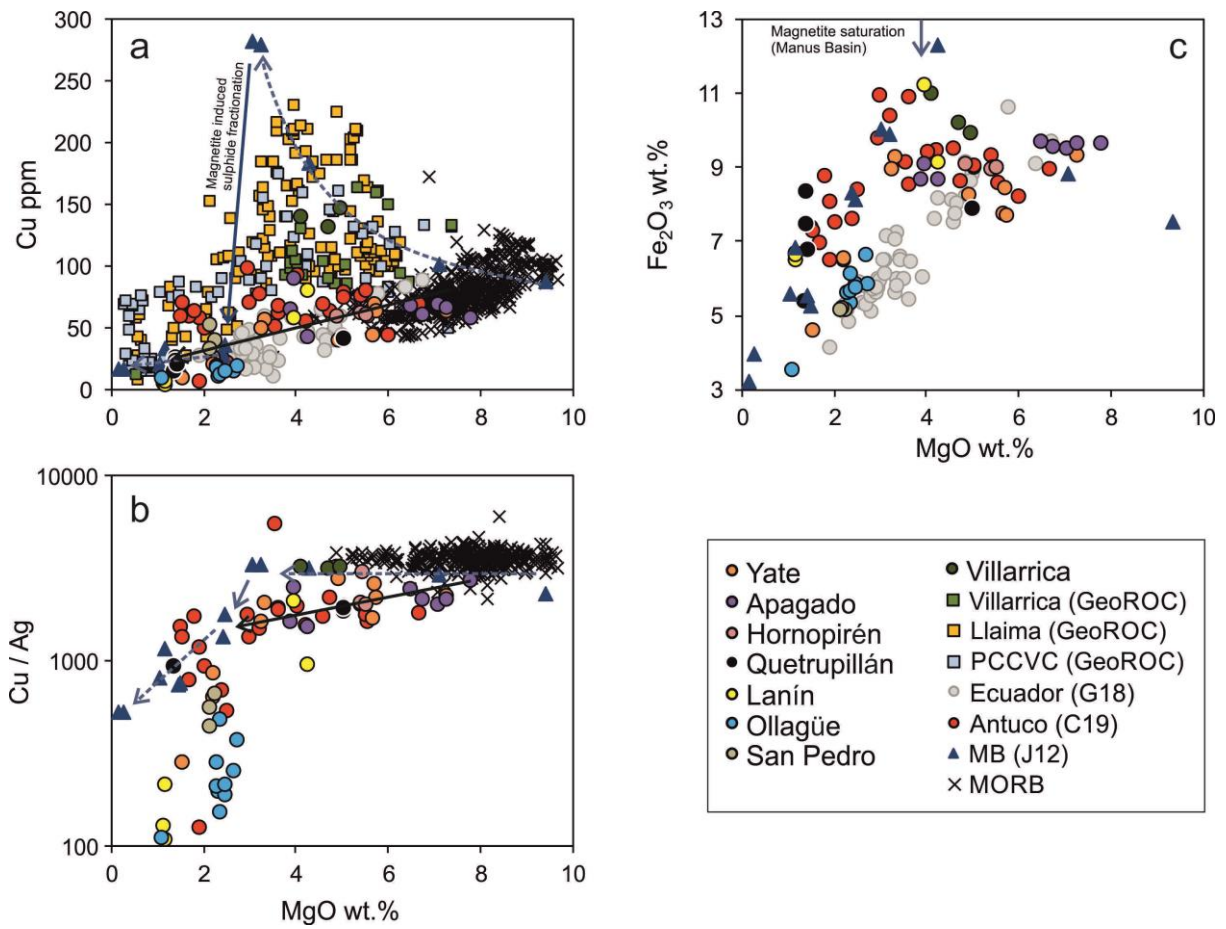


'Elevated magma fluxes deliver high-Cu magmas to the upper crust'

338 Figure 2

339

340



'Elevated magma fluxes deliver high-Cu magmas to the upper crust'

341 Figure 3

342

